Synlett M. Shevlin et al. Cluster

Concise Synthesis of Furo[2,3-*b*]indolines via [3,3]-Sigmatropic Rearrangement of *N*-Alkenyloxyindoles

Michael Shevlin[a,b]
Neil A. Strotman[a]
Laura L. Anderson*[b]

[a] Department of Process Research & Development, Merck & Co., Inc., 126 E Lincoln Ave, Rahway, NJ 07065, USA
[b] Department of Chemistry, University of Illinois at Chicago, 845 W Taylor St, Chicago, IL 60607, USA
lauralin@uic.edu

Published as part of the Cluster *Modern Heterocycle Synthesis and Functionalization*

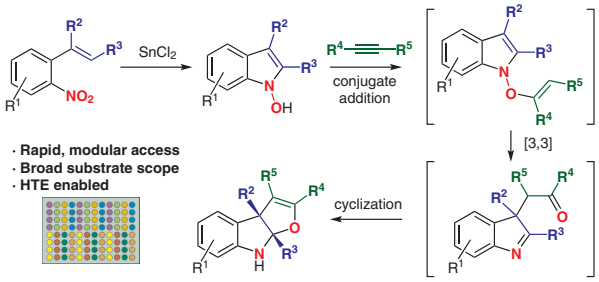

Received: 01.06.2020
Accepted after revision: 21.07.2020
Published online: 27.08.2020
DOI: 10.1055/s-0040-1707250; Art ID: st-2020-r0328-c

Crowd-Reviewed

Abstract A concise new synthetic route to furo[2,3-*b*]indolines has been developed by taking advantage of the reactivity of *N*-alkenyloxyindole intermediates. These compounds spontaneously undergo [3,3]-sigmatropic rearrangement followed by cyclization to form hemiaminals as single diastereomers. Tin-promoted *N*-hydroxyindole formation followed by conjugate addition to activated alkynes provides simple and modular access to a diverse array of *N*-alkenyloxyindoles and their corresponding furo[2,3-*b*]indolines. Microscale high-throughput experimentation was used to facilitate investigation of the scope and tolerance of this transformation and related studies on the nucleophilic aromatic substitution and rearrangement of *N*-hydroxyindoles with halogenated arenes have also been evaluated.

Key words *N*-hydroxyindole, [3,3]-sigmatropic rearrangement, heterocycle, hemiaminal, high-throughput experimentation

Heterocyclic hemiaminals are important structural motifs in organic molecules.[1] The heterocyclic hemiaminal furo[2,3-*b*]indoline motif in particular has captured the imagination of the synthetic chemistry community on account of its prevalence in natural products[2] and the pharmaceutical compounds they inspire.[3] Numerous synthetic strategies have been employed in the synthesis of furo[2,3-*b*]indolines.[4] Representative approaches include cyclization of a tethered alcohol with imine or iminium intermediates derived from oxindoles[2b] and tryptohols[2c] or cyclization of an aniline with a lactol-derived oxocarbenium ion intermediate (Scheme 1, A).[5] While these routes have been used to efficiently access simple furo[2,3-*b*]indolines, the additional synthetic steps required to prepare functionalized starting materials decreases their generality. One approach to the synthesis of these heterocycles that has remained unexplored is sigmatropic rearrangement, due to challenges in generating and controlling the reactivity of the appropriate precursors.[6–9] We hypothesized that [3,3]-sigmatropic rearrangement of *N*-alkenyloxyindoles followed by cyclization of the resulting 3*H*-indole ketone would provide a rapid, modular entry into densely functionalized compounds (Scheme 1, B). This approach is attractive because it has the potential to direct the energy of N–O bond cleavage during [3,3]-sigmatropic rearrangement towards quaternary center formation and dearomatization of the indole nucleus.[10,11] We recently reported that *N*,*O*-dialkenylhydroxylamines undergo [3,3]-sigmatropic rearrangement to form γ-ketoimines that spontaneously cyclize to 2-aminotetrahydrofuran derivatives.[12] Due to our ongoing interest in developing the synthetic utility of unsaturated hydroxylamines and nitrones, we were curious to determine if similar reactivity would be observed for *N*- alkenyloxyindoles. Herein, we report the conjugated addition of *N*-hydroxyindoles to activated alkynes resulting in rapid [3,3]-sigma-

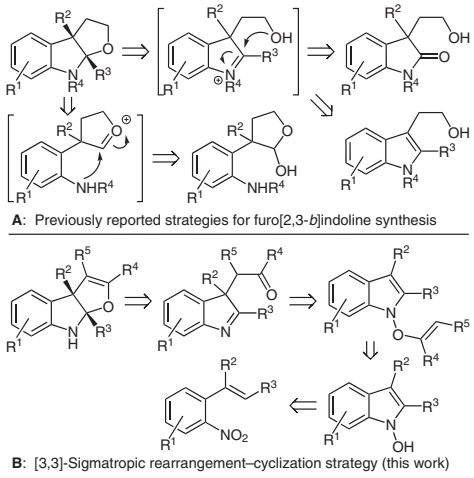

Scheme 1 Strategies for furo[2,3-*b*]indoline synthesis

Georg Thieme Verlag KG, Rüdigerstraße 14, 70469 Stuttgart, Germany

tropic rearrangement and cyclization to form furo[2,3-*b*]indolines. Microscale high-throughput experimentation (HTE) was employed to rapidly survey the scope and limitations of this new process, which provides facile and modular access to a variety of these important heterocycles.

To support our investigation of *N*-alkenyloxyindoles as key intermediates for the synthesis of furo[2,3-*b*]indolines, a range of *N*-hydroxyindoles were prepared by $SnCl_2$-mediated reductive cyclization of 2-nitrostyrenes (Scheme 2).[13] With these precursors in hand, we began screening conditions for the conjugate addition of **2b** to propiolate **3a** (Table 1). Using insight from a related synthesis of phenyl alkenyl ethers, we were initially gratified to observe the formation of **4ba** in 51% yield (Table 1, entry 1).[14] Variation of reaction conditions by switching the solvent to DMSO, changing the base to K_2CO_3, lowering the reaction temperature, and decreasing the number of equivalents of base, all enabled a gradual increase in yield (entries 2–8). DMSO was replaced with DMF to better accommodate lower reaction temperatures (entry 9) and KO*t*-Bu was observed to give similar results to K_2CO_3 (entry 10). A small additional increase in yield was observed with further lowering of reaction temperature, albeit at the expense of reaction time (entry 11). Finally, the stoichiometry of the alkyne was shown to have no significant effect on the yield of **4ba** (entry 12).

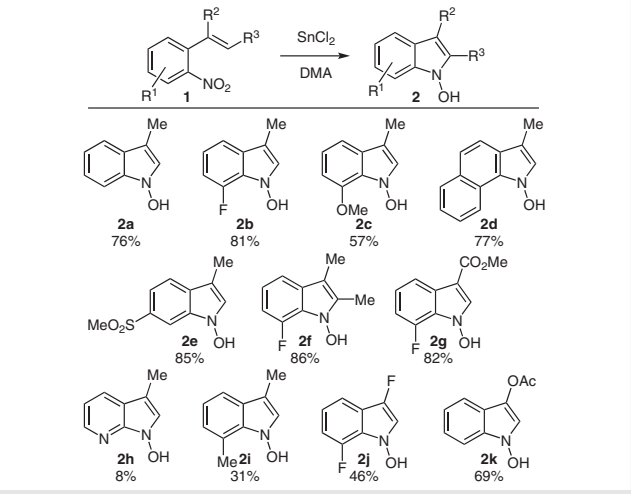

Scheme 2 Sn-promoted synthesis of *N*-hydroxyindoles from 2-nitrostyrenes

Having established optimal conditions for the desired cascade reaction, we decided to explore the scope of this transformation. To rapidly establish a broad understanding of the interactions between diversely substituted *N*-hydroxyindoles and activated alkynes, we turned to microscale HTE.[15] While HTE is routinely employed for discovery and optimization of novel reactivity, this tool has rarely been employed to study the scope of new chemical transformations.[16] In this context, HTE has the potential to examine all possible combinations of reaction partners and reveal synergies that lead to high yield and problematic combinations that give poor results.

Table 1 Optimization of Conjugate Addition/Rearrangement Conditions

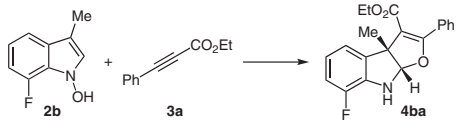

Entry	Solvent	Base	Base (equiv)	Alkyne (equiv)	Temp (°C)	Yield (%)[a]
1	MeCN	DABCO	1	1.2	70	51
2	MeCN	DABCO	1	1.2	40	39
3	MeCN	K_2CO_3	1	1.2	40	59
4	DMSO	K_2CO_3	1	1.2	40	62
5	DMSO	K_2CO_3	0.5	1.2	40	62
6	DMSO	K_2CO_3	0.2	1.2	40	61
7	DMSO	K_2CO_3	0.2	1.2	25	64
8	DMSO	K_2CO_3	0.2	2	0	69
9	DMF	K_2CO_3	0.2	2	0	69
10	DMF	KO*t*-Bu	0.2	2	0	69
11	DMF	KO*t*-Bu	0.2	2	–15[b]	74
12	DMF	KO*t*-Bu	0.2	1	0	70

[a] HPLC yield calculated as HPLC area percent at 210 nm.
[b] Reaction time 3 d.

We examined an array of eight *N*-hydroxyindoles with eight activated alkynes (Figure 1). To our delight, good to excellent yields were observed in a majority of combinations. In general, the more electron-rich *N*-hydroxyindoles **2b**, **2c**, **2d**, and **2i** gave higher yields than electron-deficient *N*-hydroxyindoles **2e**, **2g**, and **2h**. These results suggest that the increasing the nucleophilicity of the *N*-hydroxyindole leads to higher yield, perhaps by increasing the rate of the desired conjugate addition relative to competitive decomposition pathways. This hypothesis was also supported by the observation of slower reactions using mesyl-substituted hydroxyindole **2e** despite having minimal steric hindrance in the vicinity of the reaction center. 2,3-Dimethyl-substituted substrate **2f** gave somewhat lower yields due to increased steric bulk, but nicely demonstrated the ability to form products with two adjacent quaternary centers. Additional experiments with *N*-hydroxyindoles **2j** and **2k** did not result in product formation. Control experiments revealed that these substrates decomposed in the presence of base, suggesting that heteroatom substitution at the 3-position leads to substrate instability. A wide variety of activated alkynes were also tolerated in the cascade reaction array. Aryl-substituted alkynes **3a**, **3d**, **3e**, and **3f** gave higher yields than the less hindered Me-substituted alkyne **3b** and CF_3-substituted alkyne **3h**, possibly due to stabilization of

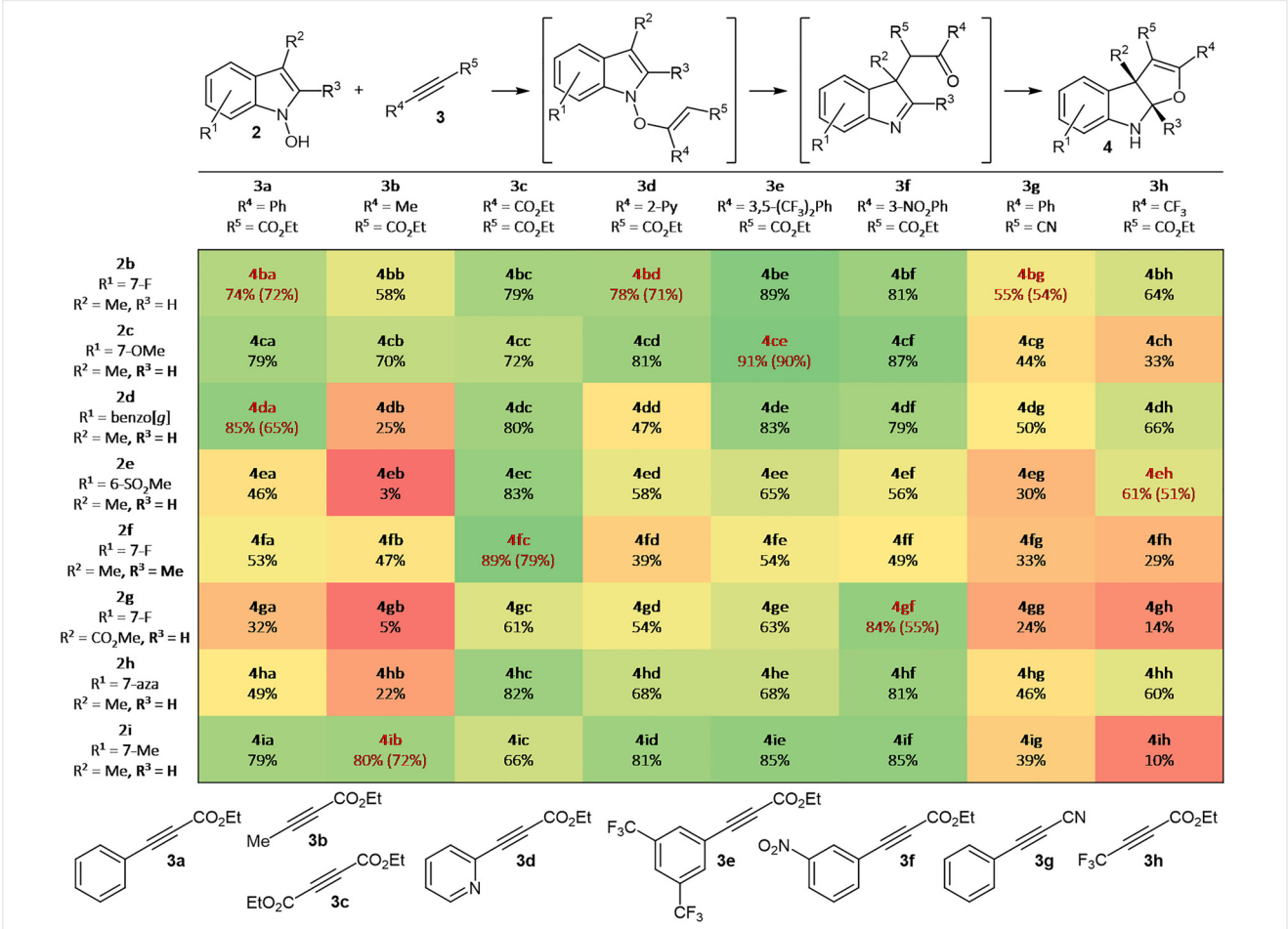

Figure 1 Substrate scope for synthesis of furo[2,3-*b*]indolines **4** from *N*-hydroxyindoles **2** and alkynes **3**. Reaction conditions: 20 µmol **2**, 1.05 equiv **3**, 20 mol% KO*t*-Bu, DMF, 0.1 M, 0 °C. Yields of isolated compounds given in parentheses are from 1 mmol scale reactions under identical conditions.

the product alkenyl ether via conjugation. Diester **3c** tended to give high product yields, highlighting its high electrophilicity. Nitrile **3g** was also tolerated, though yields were lower presumably due to competitive 1,2-addition or anionic polymerization. Neither *N*-alkenyloxyindole nor 3*H*-indole intermediates were ever observed, suggesting that conjugate addition is the rate-limiting step in this reaction cascade. A cross section of nine substrates were selected for scale-up and isolation (highlighted in red). Gratifyingly, these experiments showed that microscale HTE experiments provided reasonable guidelines for viable synthesis.

Encouraged by the success of activated alkyne electrophiles, we hypothesized that electron-deficient halogenated arenes might also be competent cascade reaction partners via S_NAr substitution, [3,3]-sigmatropic rearrangement, and cyclization sequence. We were excited to observe that the combination of *N*-hydroxyindoles **2i** or **2b** with 2-fluoro-4-cyanopyridine or 2,5- difluoropyridine gave the expected fused heterocyclic products **5** and **6**, respectively, following the S_NAr substitution, [3,3]-sigmatropic rearrangement, and cyclization sequence (Scheme 3, A). These results emphasize the utility of this new method to access heteroatom-substituted derivatives of the benzofuro[2,3-*b*]indoline core structure of natural products and pharmaceuticals.[2a,3a] Reaction of *N*-hydroxyindoles **2d** or **2f** with 2,6-dichloroquinoxaline or 2-fluoro-5-cyanopyridine gave 3*H*-indole products **7** and **8**, respectively, via S_NAr substitution and [3,3]-sigmatropic rearrangement (Scheme 3, B). These observations support the proposed [3,3]-sigmatropic rearrangement–cyclization reaction sequence and suggest that hemiaminal cyclization may be an equilibrium which is influenced by subtle changes in electronics. A combination of *N*-hydroxyindole **2g** with 2,5-difluoropyridine provided *N*-aryloxyindole product **9** which was inert toward [3,3]-sigmatropic rearrangement under the reaction conditions (Scheme 3, C), potentially due to the very electron-deficient nature of the fluoropyrimidine. Finally, substrate **2b** reacted with 2-bromo-1,4-naphthoquinone to

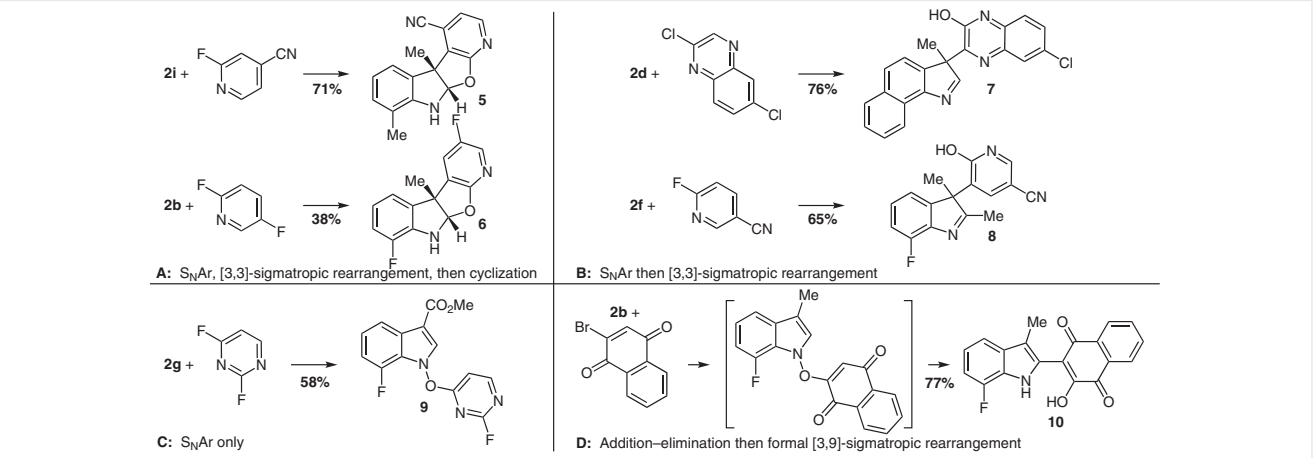

Scheme 3 Survey of reactivity of *N*-alkenyloxyindoles with halogenated arenes

give the unexpected product **10**, which can be regarded as an unusual example of a formal [3,9]-sigmatropic rearrangement (Scheme 3, D).[17]

In conclusion, we have demonstrated that formation of *N*-alkenyloxyindole intermediates allows an energetic N–O bond cleavage to drive dearomatization and quaternary center formation, resulting in a modular, concise synthesis of furo[2,3-*b*]indolines. *N*-Hydroxyindoles were synthesized from 2-nitrostyrenes via a tin-mediated reductive cyclization and upon treatment with activated alkynes, these compounds underwent conjugate addition followed by rapid [3,3]-sigmatropic rearrangement and cyclization.[18,19] Rapid substrate scope exploration was achieved with microscale HTE experiments and underscored the utility of this important tool for facilitating comprehensive reaction tolerance studies. Analogous experiments combining *N*-hydroxyindoles with electron-deficient heteroarenes revealed the subtle effects of substitution on the ability of *N*-aryloxyindoles to undergo [3,3]-sigmatropic rearrangement and subsequent cyclization. We anticipate this new method will be a useful tool in synthetic studies of biologically active furo[2,3-*b*]indoline pharmacophores.

Funding Information

National Science Foundation (CHE-1855833 to L. L. Anderson at University of Illinois at Chicago).

Acknowledgment

We gratefully acknowledge Ryan Cohen (Merck Sharp & Dohme Corp., Rahway, NJ, USA) for assistance with structure elucidation and high-resolution mass spectrometry and Artis Klapars (MSD) and Rebecca Ruck (MSD) for helpful discussion.

Supporting Information

Supporting information for this article is available online at https://doi.org/10.1055/s-0040-1707250.

References and Notes

(1) (a) Tomasz, M. *Chem. Biol.* **1995**, *2*, 575. (b) Baggaley, K. H.; Brown, A. G.; Schofield, C. J. *Nat. Prod. Rep.* **1997**, *14*, 309. (c) Behenna, D. C.; Stockdill, J. L.; Stoltz, B. M. *Angew. Chem. Int. Ed.* **2008**, *47*, 2365. (d) Ramírez, A.; Garcia-Rubio, S. *Curr. Med. Chem.* **2003**, *10*, 1891.

(2) (a) Nicolaou, K. C.; Chen, D. Y.-K.; Huang, X.; Ling, T.; Bella, M.; Snyder, S. A. *J. Am. Chem. Soc.* **2004**, *126*, 12888. (b) Matsuura, T.; Overman, L. E.; Poon, D. J. *J. Am. Chem. Soc.* **1998**, *120*, 6500. (c) Sunazuka, T.; Hirose, T.; Shirahata, T.; Harigaya, Y.; Hayashi, M.; Komiyama, K.; Ōmura, S.; Smith, A. B. *J. Am. Chem. Soc.* **2000**, *122*, 2122. (d) Teng, M.; Zi, W.; Ma, D. *Angew. Chem. Int. Ed.* **2014**, *53*, 1814.

(3) (a) Ding, H.; deRoy, P. L.; Perreault, C.; Larivée, A.; Siddiqui, A.; Caldwell, C. G.; Harran, S.; Harran, P. G. *Angew. Chem. Int. Ed.* **2015**, *54*, 4818. (b) Wang, C. H.; Alluri, S.; Nikogosyan, G.; DeCarlo, C.; Monterio, C.; Mabagos, G.; Feng, H. H.; White, A. R.; Bartolini, M.; Andrisano, V.; Zhang, L. K.; Ganguly, A. K. *Tetrahedron Lett.* **2016**, *57*, 3046. (c) Kikuchi, H.; Ichinohe, K.; Kida, S.; Murase, S.; Yamada, O.; Oshima, Y. *Org. Lett.* **2016**, *18*, 5948. (d) Luo, W.; Yu, Q.; Kulkarni, S. S.; Parrish, D. A.; Holloway, H. W.; Tweedie, D.; Shafferman, A.; Lahiri, D. K.; Brossi, A.; Grieg, N. H. *J. Med. Chem.* **2006**, *49*, 2174.

(4) For a recent review, see: Kaur, R.; Kappor, Y.; Manjal, S. K.; Rawal, R. K.; Kumar, K. *Curr. Org. Synth.* **2019**, *16*, 342.

(5) Takano, S.; Moriya, M.; Ogasawara, K. *J. Org. Chem.* **1991**, *56*, 5982.

(6) For reviews and recent examples of sigmatropic rearrangements of unsaturated hydroxylamines see: (a) Anderson, L. L. In *Molecular Rearrangements in Organic Synthesis*; Rojas, C. M., Ed.; John Wiley & Sons: Hoboken, **2015**, 431–458. (b) Tabolin, A. A.; Ioffe, S. L. *Chem. Rev.* **2014**, *114*, 5426. (c) Guo, L.; Liu, F.; Wang, L.; Yuan, L.; Feng, L.; Kürti, L.; Gao, H. *Org. Lett.* **2019**, *21*, 2894. (d) Yuan, H.; Du, Y.; Liu, F.; Guo, L.; Sun, Q.; Feng, L.; Gao, H. *Chem. Commun.* **2020**, *56*, 8226.

(7) For selected examples of related [3,3]-sigmatropic rearrangement/cyclization cascades, see: (a) Lovato, K.; Bhakta, U.; Ng, Y. P.; Kürti, L. *Org. Biomol. Chem.* **2020**, *18*, 3281. (b) Gao, H.; Xu, Q.-L.; Keene, C.; Kürti, L. *Chem. Eur. J.* **2014**, *20*, 8883. (c) Contiero, F.; Jones, K. M.; Matts, E. A.; Porzelle, A.; Tomkinson, N. C. O. *Synlett* **2009**, 3003. (d) Wang, H.-Y.; Mueller, D. S.; Sachwani, R. M.; Kapadia, R.; Londino, H. N.; Anderson, L. L. *J. Org. Chem.* **2011**, *76*, 3203. (e) Wen, J.-J.; Tang, H.-T.; Xiong, K.; Ding, Z.-C.; Zhan, Z.-P. *Org. Lett.* **2014**, *16*, 5940.

(8) For an example of a [3,3]-sigmatropic rearrangement of *N*-alkenyloxybenzotriazoles that proceeds via bond formation at C7 rather than N3, see: Kumar, M.; Scoble, M.; Mashuta, M. S.; Hammond, G. B.; Xu, B. *Org. Lett.* **2013**, *15*, 724.

(9) For examples of [3,3]-sigmatropic rearrangements of *N*-alkenyloxyindoles have been previously reported to give low yields due to competing byproduct formation, see: Duarte, M. P.; Mendonça, R. F.; Prabhakar, S.; Lobo, A. M. *Tetrahedron Lett.* **2006**, *47*, 1173.

(10) For a related transformation that uses N–O bond cleavage in a [3,3]-sigmatropic rearrangement to drive quaternary center formation in spirocyclic pyrrolines, see: Alshreimi, A. S.; Zhang, G.; Reidl, T. W.; Peña, R. L.; Koto, N.-G.; Islam, S. M.; Wink, D. J.; Anderson, L. L. *Angew. Chem. Int. Ed.* **2020**, *132*, 15356.

(11) For other examples of dearomative [3,3]-sigmatropic rearrangements that install quaternary centers, see: (a) An, J.; Parodi, A.; Monari, M.; Reis, M. C.; Lopez, C. S.; Bandini, M. *Chem. Eur. J.* **2017**, *23*, 17473. (b) Gutierrez, O.; Hendrick, C. E.; Kozlowski, M. C. *Org. Lett.* **2018**, *20*, 6539. (c) Zhao, W.; Huang, X.; Zhan, Y.; Zhang, Q.; Li, D.; Zhang, Y.; Kong, L.; Peng, B. *Angew. Chem. Int. Ed.* **2019**, *58*, 17210. (d) Peruzzi, M. T.; Lee, S. J.; Gagné, M. R. *Org. Lett.* **2017**, *19*, 6256. (e) Huang, S.; Kötzner, L.; Kanta De, C.; List, B. *J. Am. Chem. Soc.* **2015**, *137*, 3446. (f) Cao, T.; Linton, E. C.; Deitch, J.; Berritt, S.; Kozlowski, M. C. *J. Org. Chem.* **2012**, *77*, 11034. (g) Susick, R. B.; Morrill, L. A.; Picazo, E.; Garg, N. K. *Synlett* **2017**, *28*, 1. (h) Simmons, B. J.; Hoffmann, M.; Champagne, P. A.; Picazo, E.; Yamakawa, K.; Morrill, L. A.; Houk, K. N.; Garg, N. K. *J. Am. Chem. Soc.* **2017**, *139*, 14833.

(12) Son, J.; Reidl, T. W.; Kim, K. H.; Wink, D. J.; Anderson, L. L. *Angew. Chem. Int. Ed.* **2018**, *57*, 6597.

(13) (a) Shevlin, M.; Guan, X.; Driver, T. G. *ACS Catal.* **2017**, *7*, 5518. (b) Nicolaou, K. C.; Lee, S. H.; Estrada, A. A.; Zak, M. *Angew. Chem. Int. Ed.* **2005**, *44*, 3736. (c) Li, B.; Williams, J. D.; Peet, N. P. *Tetrahedron Lett.* **2013**, *54*, 3124.

(14) Stewart, G. W.; Shevlin, M.; Gammack Yamagata, A. D.; Gibson, A. W.; Keen, S. P.; Scott, J. P. *Org. Lett.* **2012**, *14*, 5440.

(15) For recent reviews, see: (a) Shevlin, M. *ACS Med. Chem. Lett.* **2017**, *8*, 601. (b) Krska, S. W.; DiRocco, D. A.; Dreher, S. D.; Shevlin, M. *Acc. Chem. Res.* **2017**, *50*, 2976.

(16) For recent examples, see: (a) Larson, H.; Schultz, D.; Kalyani, D. *J. Org. Chem.* **2019**, *84*, 13092. (b) Becica, J.; Hruszkewycz, D. P.; Steves, J. E.; Elward, J. M.; Leitch, D. C.; Dobereiner, G. E. *Org. Lett.* **2019**, *21*, 8981. (c) Cernak, T.; Gesmundo, N. J.; Dykstra, K.; Yu, Y.; Wu, Z.; Shi, Z.-C.; Vachal, P.; Sperbeck, D.; He, S.; Murphy, B. A.; Sonatore, L.; Williams, S.; Madeira, M.; Verras, A.; Reiter, M.; Lee, C. H.; Cuff, J.; Sherer, E. C.; Kuethe, J.; Goble, S.; Perrotto, N.; Pinto, S.; Shen, D.-M.; Nargund, R.; Balkovec, J.; DeVita, R. J.; Dreher, S. D. *J. Med. Chem.* **2017**, *60*, 3594. (d) Grainger, R.; Heightman, T. D.; Ley, S. V.; Lima, F.; Johnson, C. N. *Chem. Sci.* **2019**, *10*, 2264.

(17) For an example of [3,9]-sigmatropic rearrangement, see: Kessler, S. N.; Neuburger, M.; Wegner, H. A. *J. Am. Chem. Soc.* **2012**, *134*, 17885.

(18) **Synthesis of 2b – Typical Procedure**

To a 40 mL vial equipped with a magnetic stirbar, 4.26 g (23.5 mmol) 1-fluoro-2-nitro-3-(prop-1-en-2-yl)benzene, 4.90 g (25.9 mmol, 1.1 equiv) $SnCl_2$, and 25 mL DMA were added to give a homogeneous pale yellow solution. The mixture was heated to 80 °C with stirring overnight, then transferred to a 1 L separatory funnel containing 500 mL 10 wt% tartaric acid and extracted three times with MTBE. The combined organics were dried over $MgSO_4$, concentrated on a rotary evaporator, and chromatographed on a 220 g silica cartridge with a 2–20% EtOAc/hexane gradient. The desired product fractions were sequentially concentrated to approximately 50 mL volume and diluted with hexane three times. The product solution was then concentrated to approximately 10 mL volume and diluted with a small amount of MTBE (to maintain solubility) to give 9.70 g of a 32.5 wt% solution (81%). ^{1}H NMR (400 MHz, DMSO-d_6): δ = 11.28 (s, 1 H), 7.32–7.25 (m, 1 H), 7.24 (q, *J* = 1.1 Hz, 1 H), 6.98–6.85 (m, 2 H), 2.22 (d, *J* = 1.1 Hz, 3 H). ^{13}C{^{1}H} NMR (101 MHz, DMSO-d_6): δ = 148.35 (d, *J* = 244.4 Hz), 128.31 (d, *J* = 4.9 Hz), 125.62, 121.65 (d, *J* = 9.6 Hz), 118.50 (d, *J* = 6.2 Hz), 114.74 (d, *J* = 3.5 Hz), 107.00 (d, *J* = 16.8 Hz), 106.06 (d, *J* = 1.8 Hz), 9.25. HRMS (ESI/QTOF): *m/z* [M – H]$^-$ calcd for C_9H_7FNO: 164.0517; found: 164.0521.

(19) **Synthesis of 4ba – Typical Procedure**

To a 20 mL vial equipped with a magnetic stirbar, 165 mg (1.0 mmol) **2b**, 10 mL DMF, and 183 mg (1.05 mmol, 1.05 equiv) **3a**. The reaction was cooled below 0 °C, and 200 µL (1 M in THF, 200 µmol, 20 mol%) KO*t*-Bu was added dropwise. The reaction was stirred for 1 h and transferred to a 250 mL separatory funnel containing 100 mL water, 10 mL saturated NH_4Cl, and MTBE. The aqueous layer was extracted twice with MTBE, and the combined organics were dried over $MgSO_4$, concentrated on a rotary evaporator, and chromatographed on a 120 g silica cartridge with a 2–20% EtOAc/hexane gradient to give 243 mg (72%) of a white solid. ^{1}H NMR (500 MHz, $CDCl_3$): δ = 7.61 (d, *J* = 7.6 Hz, 2 H), 7.46 (d, *J* = 7.5 Hz, 1 H), 7.44–7.29 (m, 3 H), 6.98–6.83 (m, 1 H), 6.83–6.69 (m, 1 H), 6.01 (d, *J* = 2.8 Hz, 1 H), 5.18 (s, 1 H), 4.19 (q, *J* = 7.1 Hz, 2 H), 1.80 (s, 3 H), 1.19 (t, *J* = 7.2 Hz, 3 H). ^{19}F{^{1}H} NMR (471 MHz, $CDCl_3$): δ = –135.67. ^{13}C{^{1}H} NMR (126 MHz, $CDCl_3$): δ = 166.14, 164.80, 148.03 (d, *J* = 240.5 Hz), 136.72 (d, *J* = 3.5 Hz), 134.33 (d, *J* = 12.5 Hz), 130.63, 130.21, 129.27, 127.53, 120.57 (d, *J* = 3.1 Hz), 120.20 (d, *J* = 5.5 Hz), 114.65 (d, *J* = 16.9 Hz), 108.81, 103.63, 59.81, 59.24 (d, *J* = 2.1 Hz), 24.01, 14.00. HRMS (ESI/QTOF): *m/z* [M + H]$^+$ calcd for $C_{20}H_{19}FNO_3$: 340.1343; found: 340.1384.